Discrete-time Output Feedback Nonlinear Control for Combined Low- and High-Frequency Disturbance Compensation

Wonhee Kim, Xu Chen, Chung Choo Chung†, Masayoshi Tomizuka

Abstract— **We present a discrete-time output feedback nonlinear control algorithm for reference tracking under both broad-band disturbances at low frequencies and narrow-band disturbances at high frequencies. A discrete-time nonlinear damping backstepping controller with an extended state observer is proposed to track the desired output and to compensate for low-frequency broad-band disturbances. A narrow-band disturbance observer is constructed for rejecting narrow-band high-frequency disturbances. This combination method gives us the merit that both broad-band disturbances at low frequencies and narrow-band disturbances at high frequencies can be simultaneously compensated.**

I. Introduction

A robust control design for systems affected by disturbances is a fundamental issue in control engineering. One approach that has been extensively studied for disturbance rejection is to use an extended state observer (ESO) [1], [2]. By regarding the disturbance as an extended state, the system states and disturbance can be estimated using output feedback. It has been shown that the transfer function between the disturbance and the disturbance estimation error is in the form of a high pass filter [2], which provides the capability to estimate disturbances whose frequencies are below the observer bandwidth. A high observer gain is required to estimate high-frequency disturbances in ESO. Yet, this will tend to amplify measurement noises at high frequencies. Thus, it is difficult for ESO based method to compensate for the high frequency disturbances. Generally, many high frequency disturbances are in the form of induced vibrations [3], [4]. To reject this disturbance, the internal model principle (IMP) [6] based perspective has been investigated in feedback control algorithms [7], [8]. These methods are effective to cancel narrow-band disturbances, but less effective for broad-band disturbance attenuation.

In this paper, we present an output feedback nonlinear control to track the desired output with attenuation of both broad-band disturbances at low frequencies and narrow-band disturbance at high frequencies. The proposed method consists of two main parts: (i) a narrow-band disturbance observer (DOB) and (ii) a nonlinear damping backstepping controller with ESO. High-frequency disturbances are usually challenging to compensate in regular servo control. The DOB constructed based on infinite impulse response (IIR) filters [5], [9] is applied to reject the narrow-band disturbance at high frequencies. Compared to other IMP based algorithms, DOB is a convenient addition to the ESO-based backstepping control, as the former can selectively reject disturbances without altering the nominal plant dynamics, which is needed in (ii). With the functionality of DOB, the plant with mixed disturbances can be regarded as a nominal plant with just broad-band disturbances at low frequencies. The nonlinear damping backstepping controller with ESO is then proposed for tracking control and broad-band disturbance compensation. To improve servo performance when the tracking error is large, nonlinear damping is implemented in the backstepping controller. Another contribution of the paper compared to [2] and general continuous-time ESO algorithms, is the new direct discrete-time design of the nonlinear backstepping control, with proofs of stability and convergence directly in the discrete-time domain.

The proposed method was validated via simulation for a motion control problem using linear motors and air bearings.

II. Selective Model Inversion for High-frequency Disturbance Rejection

This section discusses a discrete-time internal disturbance observer for cancellation of the high-frequency disturbances using selective model inversion [5], [9].

Let the plant dynamics be modeled as

$$\frac{Y\left(z^{-1}\right)}{U\left(z^{-1}\right)} = P\left(z^{-1}\right) \tag{1}$$

where $U\left(z^{-1}\right)$ is the Z transform of the system input $u(k)$, $Y\left(z^{-1}\right)$ is the Z transform of the system output $y(k)$, The structure of the disturbance observer is shown in Fig. 1. Here, $z^{-m}P_n\left(z^{-1}\right)$ is the nominal plant model that is used in model-based feedback and feedforward designs; and m is the relative degree of the nominal model.

Remark: Note the difference between $u(k)$ and $u^*(k)$. $u^*(k)$ is the control command from the backstepping algorithm that will be later designed.

Define the Z transforms of $y(k)$, $d(k)$, and $u^*(k)$, as $Y\left(z^{-1}\right)$, $D\left(z^{-1}\right)$, $U^*\left(z^{-1}\right)$, respectively. Block-diagram analysis gives

$$Y\left(z^{-1}\right) = G_{yd}\left(z^{-1}\right)D\left(z^{-1}\right) + G_{yu^*}\left(z^{-1}\right)U^*\left(z^{-1}\right)$$

†: Corresponding Author

W. Kim is with the Department of Electrical Engineering, Dong-A University, Busan 604-714, Korea (e-mail: whkim79@dau.ac.kr)

X. Chen is with the Department of Mechanical Engineering, University of Connecticut, Storrs, CT 06269-3139, USA. (E-mail: xchen@engr.uconn.edu)

C. C. Chung is with the Division of Electrical and Biomedical Engineering, Hanyang University, Seoul, 133-791, Korea (e-mail: cchung@hanyang.ac.kr) Tel: +82-2-2220-1724, Fax: +82-2-2291-5307

M. Tomizuka is with the Department of Mechanical Engineering, University of California, Berkeley, CA 94720-1740, USA. (E-mail: tomizuka@me.berkeley.edu)

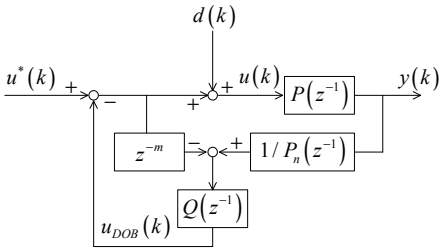

Fig. 1. Structure of the DOB

where

$$G_{yu^*}(z^{-1}) = \frac{P(z^{-1})}{1 - z^{-m}Q(z^{-1}) + P(z^{-1})P_n^{-1}(z^{-1})Q(z^{-1})} \tag{2}$$

$$G_{yd}(z^{-1}) = \frac{P(z^{-1})(1 - z^{-m}Q(z^{-1}))}{1 - z^{-m}Q(z^{-1}) + P(z^{-1})P_n^{-1}(z^{-1})Q(z^{-1})} \tag{3}$$

If $z^{-m}Q(z^{-1}) \approx 1$, then

$$G_{yu^*}(z^{-1}) \approx z^{-m}P_n(z^{-1}) \tag{4}$$

$$G_{yd}(z^{-1}) \approx 0 \tag{5}$$

namely, the plant uncertainty and the disturbance $d(k)$ are rejected in the local feedback loop, such that the overall dynamics between $u^*(k)$ and $y(k)$ approximately equals the nominal model $z^{-m}P_n(z^{-1})$.

If $Q(z^{-1}) \approx 0$, then

$$G_{yu^*}(z^{-1}) = G_{yd}(z^{-1}) = P(z^{-1}) \tag{6}$$

and DOB is disengaged from the loop.

When combined with the nonlinear damping backstepping control, it is desired that

i) (4) is valid in a large frequency range, and
ii) (5) holds at frequencies where strong external disturbances occur outside the control bandwidth of the backstepping design.

For precision systems, good model information is usually available such that $P \approx z^{-m}P_n(z^{-1})$ in a large region [satisfaction of i)]. High-frequency disturbances however are usually challenging to compensate in regular servo control [challenge in ii)]. Assume the high-frequency disturbance is centered at ω_d (in rad/sec), the DOB can be designed as follows: let

$$Q(z^{-1}) = [Q_o(z^{-1})]^m$$

where

$$Q_o(z^{-1}) = (\alpha - 1)\frac{(\alpha + 1)z^{-1} - 2\cos(\omega_d T_s)}{1 - 2\alpha\cos(\omega_d T_s)z^{-1} + \alpha^2 z^{-2}}$$

This way, the Q filter has the frequency response as shown in Fig. 2. Such a Q-filter design achieves $z^{-m}Q(z^{-1})\big|_{z=e^{j\omega_d T_s}} = 1$. From (5), $G_{yd}(z^{-1})\big|_{z=e^{j\omega_d T_s}}$ thus equals zero, namely, we achieve perfect disturbance rejection at the particular frequency ω_d. At frequencies other than ω_d, Q has small gains and the system recovers to (6), hence maintaining

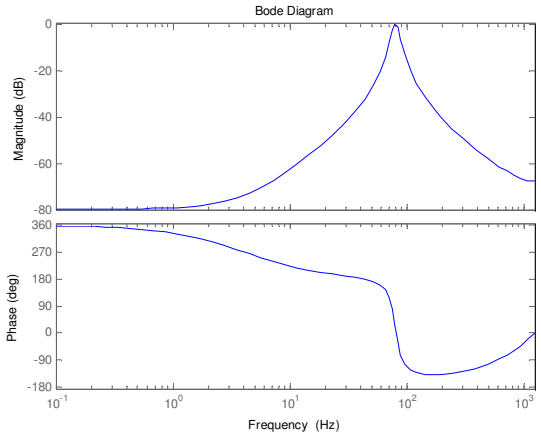

Fig. 2. Frequency response of an example Q filter

the original dynamic properties. Analogous design can be applied for the case of disturbance rejection at multiple frequencies [5], [9].

Stability of the disturbance-observer loop: From (2) and (3), the poles of the local disturbance observer loop contain

- poles of $Q(z^{-1})$, and
- roots of

$$1 - z^{-m}Q(z^{-1}) + P(z^{-1})P_n^{-1}(z^{-1})Q(z^{-1}) = 0 \tag{7}$$

From (7), a sufficient condition for its roots to be stable is that

$$|Q(e^{-j\omega})| < \frac{1}{|P(e^{-j\omega})P_n^{-1}(e^{-j\omega}) - e^{-jm\omega}|} = \frac{1}{|\Delta(e^{-j\omega})|}$$

III. Design of Output Feedback Nonlinear Damping Backstepping Controller for Low-frequency Disturbance Rejection

This section discusses the proposed tracking control with compensation of strong external low-frequency disturbances, using an ESO and a discrete-time nonlinear damping backstepping controller for the nominal plant $z^{-m}P_n(z^{-1})$.

Let the nominal system model $z^{-m}P_n(z^{-1})$ be given by

$$z^{-m}P_n(z^{-1}) = \frac{b_{n-1}z^{n-1} + \cdots + b_1 z + b_0}{z^n + a_{n-1}z^{n-1} + \cdots + a_1 z + a_0}. \tag{8}$$

Under the assumption that the numerator and the denominator of (8) are coprime, a minimal state-space realizations of (8) can be represented as

$$\begin{aligned} x(k+1) &= Ax(k) + Bu^*(k) + Bd(k) \\ y(k) &= Cx(k) \end{aligned} \tag{9}$$

where $x(k) = \begin{bmatrix} x_1(k) & x_2(k) & \cdots & x_n(k) \end{bmatrix}^T \in \mathbb{R}^{n\times 1}$ is the state vector, $u^*(\cdot)$ is the control input, $d(\cdot)$ is the residual disturbance after narrow-band disturbance compensation.

Additionally,

$$A = \begin{bmatrix} 0 & 1 & 0 & \cdots & 0 & 0 \\ 0 & 0 & 1 & \cdots & 0 & 0 \\ \vdots & \vdots & \vdots & \ddots & \ddots & \ddots \\ 0 & 0 & 0 & \cdots & 0 & 1 \\ -a_0 & -a_1 & -a_2 & \cdots & -a_{n-2} & -a_{n-1} \end{bmatrix} \in \mathbb{R}^{n\times n}$$

$$B = \begin{bmatrix} 0_{1\times(n-1)} & 1 \end{bmatrix}^T \in \mathbb{R}^{n\times 1}$$

$$C = \begin{bmatrix} b_0 & b_1 & b_2 & \cdots & b_{n-2} & b_{n-1} \end{bmatrix} \in \mathbb{R}^{1\times n}.$$

Here, the transfer function from y to x_1 is

$$\frac{X_1(z^{-1})}{Y(z^{-1})} = \frac{1}{b_{n-1}z^{n-1} + b_{n-2}z^{n-2} + \cdots + b_1 z + b_0}, \quad (10)$$

Given a designed y_d, x_{1_d}–the desired state of x_1 (required for the controller design)–can be made from the following equation

$$X_{1_d}(z^{-1}) = \frac{1}{b_{n-1}z^{n-1} + b_{n-2}z^{n-2} + \cdots + b_1 z + b_0} Y_d(z^{-1}). \quad (11)$$

Here we assume that $d(k)$ is slowly time-varying such that

$$d(k+1) = d(k) + \delta(k). \quad (12)$$

where $|\delta(k)| \le \delta_{\max}$.

A. Design of ESO

With the disturbance $d(k)$ defined as an extended state

$$x_{n+1}(k) = d(k) \quad (13)$$

the augmented state-space plant model (10) becomes

$$\begin{aligned} x_{ex}(k+1) =& A_{ex}x_{ex}(k) + B_{ex}u^*(k) + B_d\delta(k) \\ y(k) =& C_{ex}x_{ex}(k) \end{aligned} \quad (14)$$

where $x_{ex}(k) = \begin{bmatrix} x^T(k) & x_{n+1}(k) \end{bmatrix}^T$,

$$A_{ex} = \begin{bmatrix} 0 & 1 & 0 & \cdots & 0 & 0 \\ 0 & 0 & 1 & \cdots & 0 & 0 \\ \vdots & \vdots & \vdots & \ddots & \ddots & \ddots \\ 0 & 0 & 0 & \cdots & 1 & 0 \\ -a_0 & -a_1 & -a_2 & \cdots & -a_{n-1} & 1 \\ 0 & 0 & 0 & \cdots & 0 & 1 \end{bmatrix} \in \mathbb{R}^{(n+1)\times(n+1)}$$

$$B_{ex} = \begin{bmatrix} 0_{1\times(n-1)} & 1 & 0 \end{bmatrix}^T \in \mathbb{R}^{(n+1)\times 1}$$

$$B_d = \begin{bmatrix} 0_{1\times n} & 1 \end{bmatrix}^T \in \mathbb{R}^{(n+1)\times 1}$$

$$C_{ex} = \begin{bmatrix} b_0 & b_1 & b_2 & \cdots & b_{n-1} & 0 \end{bmatrix} \in \mathbb{R}^{1\times(n+1)}.$$

We assume that the pair (A_{ex}, C_{ex}) is observable. This is true if the plant does not have a zero at $z = 1$ to cancel the disturbance mode in (12) under the assumption that the numerator and the denominator of (8) are coprime. The ESO is designed as

$$\begin{aligned} \hat{x}_{ex}(k+1) =& A_{ex}\hat{x}_{ex}(k) + B_{ex}u^*(k) + L(y(k) - \hat{y}(k)) \\ \hat{y}(k) =& C_{ex}\hat{x}_{ex}(k) \end{aligned} \quad (15)$$

where $\hat{x}_{ex} = \begin{bmatrix} \hat{x}_1 & \cdots & \hat{x}_{n+1} \end{bmatrix}^T$ is the estimated x_{ex} and $L = \begin{bmatrix} l_1 & l_2 & \cdots & l_n & l_{n+1} \end{bmatrix}^T \in \mathbb{R}^{(n+1)\times 1}$ is the observer gain matrix. Define the estimation error

$$\tilde{x}_{ex} = \begin{bmatrix} \tilde{x}_1 \\ \tilde{x}_2 \\ \vdots \\ \tilde{x}_n \\ \tilde{x}_{n+1} \end{bmatrix} = \begin{bmatrix} x_1 - \hat{x}_1 \\ x_2 - \hat{x}_2 \\ \vdots \\ x_n - \hat{x}_n \\ x_{n+1} - \hat{x}_{n+1} \end{bmatrix} \in \mathbb{R}^{(n+1)\times 1}. \quad (16)$$

Then the estimation error dynamics are

$$\tilde{x}_{ex}(k+1) = \bar{A}\tilde{x}_{ex}(k) + B_d\delta(k) \quad (17)$$

where $\bar{A} = (A_{ex} - LC_{ex})$. For stability analysis, we define the Lyapunov candidate function V_o as

$$V_o(k) = \tilde{x}_{ex}^T(k) P_o \tilde{x}_{ex}(k) \quad (18)$$

where P_o is positive definite. Since P_o is positive definite, $\zeta^T P_o \zeta \ge 0$ for any ζ. If we choose $\zeta = \sqrt{\nu}\bar{A}\tilde{x}_{ex}(k) - B_d\delta(k)/\sqrt{\nu}$, then

$$\left(\sqrt{\nu}\bar{A}\tilde{x}_{ex} - \frac{B_d\delta}{\sqrt{\nu}}\right)^T P_o \left(\sqrt{\nu}\bar{A}\tilde{x}_{ex} - \frac{B_d\delta}{\sqrt{\nu}}\right) \ge 0. \quad (19)$$

Thus, we obtain

$$\begin{aligned} &\tilde{x}_{ex}^T(k)\bar{A}^T P_o B_d\delta(k) + \delta(k)B_d^T P_o \bar{A}\tilde{x}_{ex}(k) \\ &\le \nu\tilde{x}_{ex}^T(k)\bar{A}P_o\bar{A}\tilde{x}_{ex}(k) + \frac{\delta(k)B_d^T P_o B_d\delta(k)}{\nu}. \end{aligned} \quad (20)$$

Then, $\Delta V_o(k) = V_o(k+1) - V_o(k)$ is

$$\begin{aligned} \Delta V_o(k) =& \tilde{x}_{ex}^T(k+1)P_o\tilde{x}_{ex}(k+1) - \tilde{x}_{ex}^T(k)P_o\tilde{x}_{ex}(k) \\ =& \left[\bar{A}\tilde{x}_{ex}(k) + B_d\delta(k)\right]^T P_o \left[\bar{A}\tilde{x}_{ex}(k) + B_d\delta(k)\right] \\ &- \tilde{x}_{ex}^T(k)P_o\tilde{x}_{ex}(k) \\ =& \tilde{x}_{ex}^T[\bar{A}^T P_o\bar{A} - P_o]\tilde{x}_{ex} + \tilde{x}_{ex}^T(k)\bar{A}^T P_o B_d\delta(k) \\ &+ \delta(k)B_d^T P_o\bar{A}\tilde{x}_{ex}(k) + B_d^T P_o B_d\delta^2(k). \end{aligned} \quad (21)$$

From (20) and (21),

$$\begin{aligned} \Delta V_o(k) \le& \tilde{x}_{ex}^T[(1+\nu)\bar{A}^T P_o\bar{A} - P_o]\tilde{x}_{ex} \\ &+ \left(1 + \frac{1}{\nu}\right) B_d^T P_o B_d\delta^2(k). \end{aligned} \quad (22)$$

If eigenvalues of $\bar{A} = (A_{ex} - LC_{ex})$ are all inside the unit circle, the positive definite matrix solution P_o to the Lyapunov matrix equation

$$Q_o = -[\bar{A}^T P_o\bar{A} - P_o] \quad (23)$$

exists such that Q_o is positive definite. Note that $|\lambda(\sqrt{1+\nu}\bar{A})| = \sqrt{1+\nu}|\lambda(\bar{A})|$ where $\lambda(A)$ denotes the eigenvalues of A. Replacing $\bar{A}$ by $\sqrt{1+\nu}\bar{A}$ in (23), the matrix equation

$$Q_o = -[(1+\nu)\bar{A}^T P_o\bar{A} - P_o] \quad (24)$$

has a unique positive definite solution P_o if $|\lambda(\bar{A})| < \frac{1}{\sqrt{1+\nu}}$ [12]. Consequently,

$$\begin{aligned}\Delta V_o(k) \leq & \tilde{x}_{ex}^T Q_o \tilde{x}_{ex} + \left(1+\frac{1}{\nu}\right) B_d^T P_o B_d \delta_{\max}^2(k) \\ \leq & -\lambda_{\min}(Q_o)\|\tilde{x}_{ex}\|_2^2 + \left(1+\frac{1}{\nu}\right)\|P_o\|_2 \delta_{\max}^2(k).\end{aligned} \tag{25}$$

From (25), we conclude that if $|\lambda(\bar{A})| < \frac{1}{\sqrt{1+\nu}}$, x_{ex} converges to the bounded ball $B_r = \left\{\tilde{x}_{ex} | \|\tilde{x}_{ex}\|_2 \leq \frac{\sqrt{\|P_o\|_2}\delta_{\max}}{\sqrt{\nu}\lambda_{\min}(Q_o)}\right\}$.

Analogous to the continuous-time case in [2], the transfer function $H(z)$ from the disturbance d to the estimation error $\tilde{d}$ is in the form of the high pass filter as

$$\begin{aligned}H(z) :=& \frac{\tilde{D}(s)}{D(s)} \\ =& \frac{z^r(z^n + l_1 z^{n-1} + \cdots + l_n)}{z^{n+r} + l_1 z^{n+r-1} + \cdots + l_{n+r-1} z + l_{n+r}}.\end{aligned} \tag{26}$$

Thus the extended observer can effectively estimate disturbances whose frequencies are below the cut-off frequency of $H(z)$.

B. Design of Nonlinear Damping Backstepping

For output tracking, we will design the controller via backstepping. We define the tracking error $e(k) = \begin{bmatrix} e_1(k) & e_2(k) & \cdots & e_n(k)\end{bmatrix}^T$ as

$$\begin{aligned}e_1(k) =& x_{1_d}(k) - x_1(k) \\ \vdots & \\ e_{n-1}(k) =& x_{n-1_d}(k) - x_{n-1}(k) \\ e_n(k) =& x_{n_d}(k) - x_n(k)\end{aligned} \tag{27}$$

where $x_{i_d},\ i \in [2,\ n]$ will be designed in a moment. Based on (17), the tracking error system is

$$\begin{aligned}e_1(k+1) =& x_{1_d}(k+1) - x_2(k) \\ \vdots & \\ e_{n-1}(k+1) =& x_{n-1_d}(k+1) - x_n(k) \\ e_n(k+1) =& x_{n_d}(k+1) - x_n(k+1)\end{aligned} \tag{28}$$

which can be written as

$$\begin{aligned}e_1(k+1) =& x_{1_d}(k+1) - x_{2_d}(k) + e_2(k) \\ \vdots & \\ e_{n-1}(k+1) =& x_{n-1_d}(k+1) - x_{n_d}(k) + e_n(k) \\ e_n(k+1) =& x_{n_d}(k+1) + \sum_{i=1}^{n} a_{i-1}x_i(k) - x_{n+1}(k) - u^*(k).\end{aligned} \tag{29}$$

The desired state variables and control input in the nonlinear damping backsteppig controller are designed as

$$\begin{aligned}x_{2_d}(k) =& -c_1 e_1(k) + x_{1_d}(k+1) \\ \vdots & \\ x_{n_d}(k) =& -c_{n-1}e_{n-1}(k) + x_{n_d}(k+1) \\ u^*(k) =& -c_n e_n(k) + x_{n_d}(k+1) + \sum_{i=1}^{n} a_{i-1}x_i(k) \\ & - \hat{x}_{n+1}(k) + c_d(\hat{e}_1, \hat{x}_{n+1})e_n(k)\end{aligned} \tag{30}$$

where $|c_i| < 1,\ \ i \in [1,n],\ \ c_d(\hat{e}_1, \hat{x}_{n+1}) = c_n[1 - \exp(-c_{d_1}\hat{e}_1^2(k) - c_{d_2}\hat{x}_{n+1}^2(k) - \nu)],\ c_{d_1} > 0,\ c_{d_2} > 0,\ \nu > 0$, and $\hat{e}_1 = x_{1_d} - \hat{x}_1$. In $u^*(k)$, the term $-c_n e_n(k) + x_{n_d}(k+1) + \sum_{i=1}^{n} a_{i-1}x_i(k) - \hat{x}_{n+1}(k)$ is for stabilization of the system. The term $c_n[1 - \exp(-c_{d_1}\hat{e}_1^2(k) - c_{d_2}\hat{x}_{n+1}^2(k) - \nu)]$ is the nonlinear damping term. Generally, the estimated output tracking error $\hat{e}_1(k)$ and the estimated disturbance $\hat{x}_{n+1}(k)$ increase when the disturbance estimation error $\tilde{x}_{n+1}(k)$ increases. The role of the nonlinear damping term makes the control gain $-c_n + c_d(\hat{e}_1, \hat{x}_{n+1})$ of u^* get close to zero for a large disturbance estimation error $\tilde{x}_{n+1}(k)$, which will later provide a tighter bound of the errors in (35).

With the controller (30), the tracking error system (29) becomes

$$\begin{aligned}e_1(k+1) =& c_1 e_1(k) + e_2(k) \\ \vdots & \\ e_{n-1}(k+1) =& c_{n-1}e_{n-1}(k) + e_n(k) \\ e_n(k+1) =& c_{n_s}(k)e_n(k) - \tilde{x}_{n+1}(k)\end{aligned} \tag{31}$$

where $c_{n_s}(k) = c_n - c_d(\hat{e}_1(k), \hat{x}_{n+1}(k))$. Now we show the boundedness of the tracking errors in (31) and provide equations about how the design parameters control the error bound.

From $e_n(k+1)$ in (31), we have

$$e_n(k) = \prod_{j=0}^{k-1} c_{n_s}(j)e_n(0) + \sum_{j=0}^{k-1} c_{n_s}^{k-j}(j)\tilde{x}_{n+1}(j). \tag{32}$$

Since $|c_{n_s}(k)| < 1$ for all k and $\hat{x}_{n+1}(k)$ is bounded, $e_n(k)$ is also bounded. From $e_{n-1}(k+1)$ in (31), we also have

$$e_{n-1}(k) = c_{n-1}^k e_1(0) + \sum_{j=0}^{k-1} c_{n-1}^{k-j} e_n(j). \tag{33}$$

Since $|c_{n-1}| < 1$ and $e_n(k)$ is bounded, $e_{n-1}(k)$ is also bounded. Thus, we have

$$\begin{aligned}e_1(k) =& c_1^k e_1(0) + \sum_{j=0}^{k-1} c_1^{k-j} e_2(j) \\ \vdots & \\ e_{n-1}(k) =& c_{n-1}^k e_1(0) + \sum_{j=0}^{k-1} c_{n-1}^{k-j} e_n(j) \\ e_n(k) =& \prod_{j=0}^{k-1} c_{n_s}(j)e_n(0) + \sum_{j=0}^{k-1} c_{n_s}^{k-j}(j)\tilde{x}_{n+1}(j).\end{aligned} \tag{34}$$

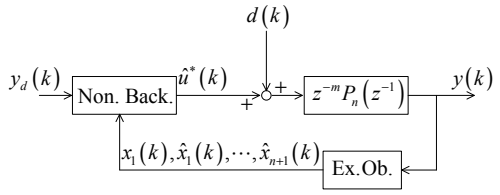

Fig. 3. Structure of the control system

Using the technique in [10], it can be derived that

$$\begin{aligned}
\lim_{k\to\infty}|e_1(k)| &\le \sup_k \frac{1}{1-|c_1|}|e_2(k)| \\
&\vdots \\
\lim_{k\to\infty}|e_{n-1}(k)| &\le \sup_k \frac{1}{1-|c_{n-1}|}|e_n(k)| \\
\lim_{k\to\infty}|e_n(k)| &\le \sup_k \frac{1}{1-|c_n-c_d(\hat{e}_1(k),\hat{x}_{n+1}(k))|}|\tilde{x}_{n+1}(k)|.
\end{aligned} \tag{35}$$

Equation (35) shows the input-to-state stability (ISS) property of the tracking error system (31). As $\hat{e}_1$ and $\hat{d}=\hat{x}_{n+1}$ get larger, $\frac{1}{1-|c_n-c_d(\hat{e}_1,\hat{x}_{n+1})|}$ gets closer to 1, yielding a smaller gain for the effect of $|\tilde{x}_{n+1}(k)|$.

C. Stability Analysis of the Closed-loop System

In practice, usually only the output y is available. The other states in (28) is replaced by its estimate $\hat{x}_i$ for implementation of (30). Thus the control law (30) becomes

$$\begin{aligned}
\hat{x}_{2_d}(k) &= -c_1\hat{e}_1(k)+x_{1_d}(k+1) \\
&\vdots \\
\hat{x}_{n_d}(k) &= -c_{n-1}\hat{e}_{n-1}(k)+\hat{x}_{n_d}(k+1) \\
\hat{u}^*(k) &= -c_n\hat{e}_n(k)+\hat{x}_{n_d}(k+1)+\sum_{i=1}^{n}a_{i-1}\hat{x}_i(k)-\hat{x}_{n+1}(k) \\
&\quad + c_n[1-\exp(-c_{d_1}\hat{e}_1^2(k)-c_{d_2}\hat{x}_{n+1}^2(k)-\nu)]\hat{e}_n(k)
\end{aligned} \tag{36}$$

where $\hat{e}_i=\hat{x}_i-\hat{x}_{i_d},\ i\in[1,n]$. Fig. 3 shows the structure of the control system that consists of the nominal plant, the ESO, and the nonlinear damping backstepping controller. Now we study the stability of the closed-loop system. The nth subsystem of the tracking error dynamics (31) becomes

$$\begin{aligned}
e_n(k+1) =& [c_n-c_d(\hat{e}_1(k),\hat{x}_{n+1}(k))]e_n(k) \\
&-\tilde{x}_{n+1}(k)+u_2^*(k)-u_1^*(k).
\end{aligned} \tag{37}$$

As shown in (31) and (37), since the observer affects only the nth subsystem of the tracking error dynamics (31), it is sufficient to investigate the behavior of the nth subsystem owing to the cascade ISS property. In $u^*(k)$ and $\hat{u}^*(k)$, the different desired state variables, x_i^d and $\hat{x}_{i_d}$ $i\in[3,n]$, are used respectively. On the other hand, x_1, x_{1_d}, and x_{2_d} are used in both (30) and (36). Thus, a positive constant γ exists such that

$$|\tilde{x}_{n+1}+\hat{u}^*-u^*|\le\gamma\|\hat{x}_{ex}-x_{ex}\|_2. \tag{38}$$

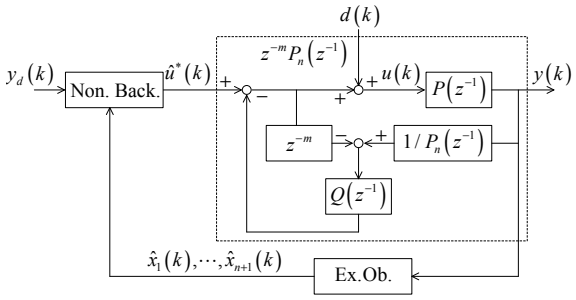

Fig. 4. Structure of the overall control system

From (37)

$$\begin{aligned}
|e_n(k+1)| \le& |(c_n-c_d(\hat{e}_1(k),\hat{x}_{n+1}(k)))e_n(k)| \\
&+|\tilde{x}_{n+1}(k)+\hat{u}^*(k)-u^*(k)|
\end{aligned} \tag{39}$$

and based on (35), e_n satisfies

$$\begin{aligned}
\lim_{k\to\infty}|e_n(k)| &\le \sup_k \frac{|\tilde{x}_{n+1}(k)+u_2^*(k)-u_1^*(k)|}{1-|c_n-c_d(\hat{e}_1(k),\hat{x}_{n+1}(k))|} \\
&\le \sup_k \frac{\gamma\|\tilde{x}_{ex}(k)\|_2}{1-|c_n-c_d(\hat{e}_1(k),\hat{x}_{n+1}(k))|}.
\end{aligned} \tag{40}$$

Finally, from (35) and (40), we have

$$\begin{aligned}
\lim_{k\to\infty}|e_1(k)| &\le \sup_k \frac{1}{1-|c_1|}|e_2(k)| \\
&\vdots \\
\lim_{k\to\infty}|e_{n-1}(k)| &\le \sup_k \frac{1}{1-|c_{n-1}|}|e_n(k)| \\
\lim_{k\to\infty}|e_n(k)| &\le \sup_k \frac{\gamma\|\tilde{x}_{ex}(k)\|_2}{1-|c_n-c_d(\hat{e}_1(k),\hat{x}_{n+1}(k))|}
\end{aligned} \tag{41}$$

Equation (41) thus shows the ISS property of the tracking error system (31) with (37).

IV. Overall Control System

Fig. 4 shows the structure of the overall control system. With DOB compensating the high-frequency disturbances, the plant with mixed disturbances can be regarded as the nominal plant with just broad-band disturbances at low frequencies.

For implementation, the output of $P(z^{-1})$ with the narrow-band DOB is used instead of that of $z^{-m}P_n(z^{-1})$ in ESO (15). The output of $z^{-m}P_n(z^{-1})$ was defined as $y=Cx=C_{ex}x_{ex}$. The actually output, the output of P with the DOB, is defined as y_{ac}. Due to the difference between y and y_{ac}, the estimation error dynamics (17) becomes

$$\tilde{x}_{ex}(k+1)=(A_{ex}-LC_{ex})\tilde{x}_{ex}(k)+B_d\Delta d(k)+L(y_{ac}(k)-y(k)). \tag{42}$$

Since the DOB guarantees the stability of the disturbance-observer loop, $y_{ac}-y$ is bounded. Thus the results from (18) to (21) give us the boundedness of the estimation error. Consequently, the ISS property of the tracking error system (31) guarantees the boundedness of the output tracking error.

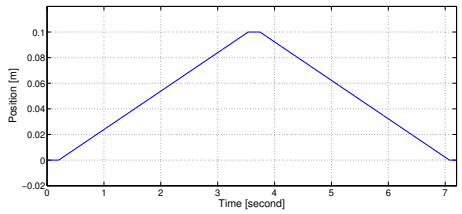

Fig. 5. The desired output y_d

V. Simulation Evaluation

This section provides applications of the algorithm to a motion control system for photolithography that has been described in [11]. It consists of linear motors and air bearings. The precision system has a quite accurate model. The transfer function of the plant is

$$P(z^{-1}) = \frac{bz+0.8b}{z^3-2z^2+z} = z^{-2}\frac{b+0.8bz^{-1}}{1-2z^{-1}+z^{-2}} \tag{43}$$

where $b = 3.4766\times 10^{-7}$. Then $m = 2$, and

$$P_n^{-1}\left(z^{-1}\right) = \frac{z^2-2z+1}{bz^2+0.8bz}.$$

A minimum state-space realizations of the plant is

$$\begin{aligned} x(k+1) &= \begin{bmatrix} 0 & 1 & 0 \\ 0 & 0 & 1 \\ 0 & -1 & 2 \end{bmatrix} x(k) + \begin{bmatrix} 0 \\ 0 \\ 1 \end{bmatrix} u(k) \\ y(k) &= \begin{bmatrix} 0.8b & b & 0 \end{bmatrix} x(k) \end{aligned} \tag{44}$$

where $x(k) = \begin{bmatrix} x_1(k) & x_2(k) & x_3(k) \end{bmatrix}^T$. The model of the plant including the disturbance is

$$\begin{aligned} x(k+1) &= \begin{bmatrix} 0 & 1 & 0 \\ 0 & 0 & 1 \\ 0 & -1 & 2 \end{bmatrix} x(k) + \begin{bmatrix} 0 \\ 0 \\ 1 \end{bmatrix} u(k) + \begin{bmatrix} 0 \\ 0 \\ 1 \end{bmatrix} d(k) \\ y(k) &= \begin{bmatrix} 0.8b & b & 0 \end{bmatrix} x(k) \end{aligned} \tag{45}$$

Using (10), x_{1_d} is obtained by

$$X_{1_d}(z^{-1}) = \frac{1}{bz+0.8b} Y_d(z^{-1}). \tag{46}$$

In these simulations, the desired output y_d is shown in Fig. 5.

For comparison, we tested three cases:

[Case 1:] w/o DOB; under disturbances at only low frequencies

[Case 2:] w/o DOB; under disturbances at both low and high frequencies

[Case 3:] w/ DOB; under disturbances at both low and high frequencies.

In the three cases, the nonlinear damping backstepping controller (30) with the ESO (15) was used. $2\sin(k)$ and $\sin(2k)$ were used as the disturbances at low frequencies; $\sin(160\pi k)$ was used as the disturbance at high frequency.

Fig 6 shows the simulation results of case 1. Since the disturbance $d = x_4$ was accurately estimated, the nonlinear damping backstepping controller (30) achieved good tracking

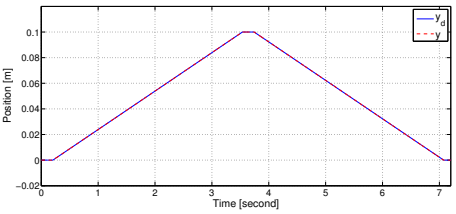

(a) Output tracking performance of y

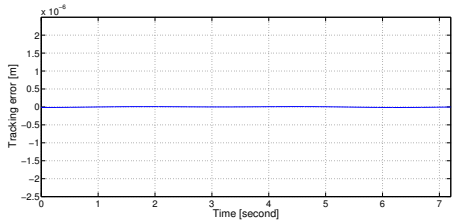

(b) Output tracking error $y_d - y$

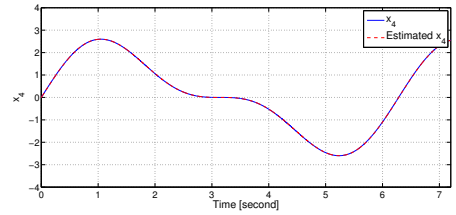

(c) Estimation performance of $d = x_4$

Fig. 6. Simulation results of case 1

of y_d. Estimation performance of case 1 is shown in Fig. 7. It is observed that the estimated state variables tracked the state variables well. The simulation results of case 2 are shown in Fig 8. Unlike case 1, the system was subjected to high-frequency disturbances whose frequency was higher than the bandwidth of ESO. Thus high-frequency ripples appeared in the output tracking error. Fig 9 shows the simulation results of case 3. With the narrow-band DOB, the high-frequency disturbance was significantly attenuated and the output tracking error of case 3 was reduced to the same level as that in case 1.

VI. Conclusions

A discrete-time output feedback nonlinear control was proposed to track the desired output with both broad-band disturbances at low frequencies and narrow-band disturbance at high frequencies. In the proposed algorithm, an ESO estimates the full state and broad-band disturbance at low frequencies; and design of a narrow-band DOB was provided to reject the narrow-band disturbance at high frequencies. Simulation results showed that the proposed method can compensate for both broad-band disturbance at low frequencies and narrow-band disturbance at high frequencies.

References

[1] M. Zeitz, "The extended Luenberger observer for nonlinear systems," *Syst. Control Lett.,* vol. 9, no. 2, pp. 149-156, 1987.

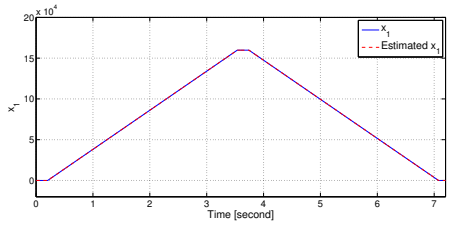

(a) Estimation performance of x_1

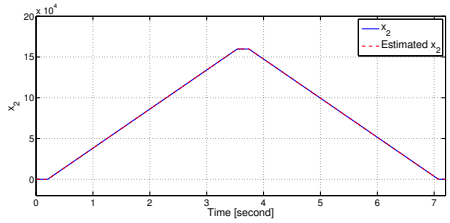

(b) Estimation performance of x_1

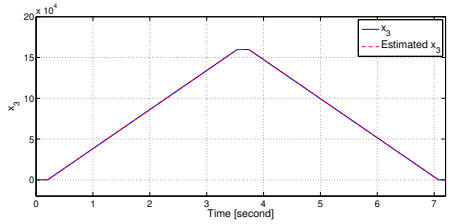

(c) Estimation performance of x_1

Fig. 7. Estimation performance of case 1

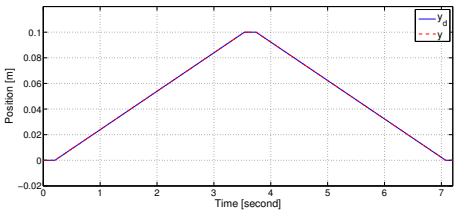

(a) Output tracking performance of y

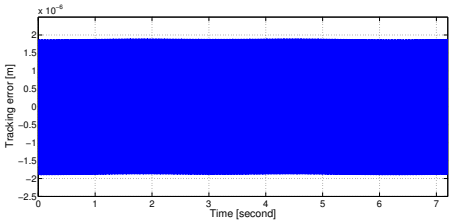

(b) Output tracking error $y_d - y$

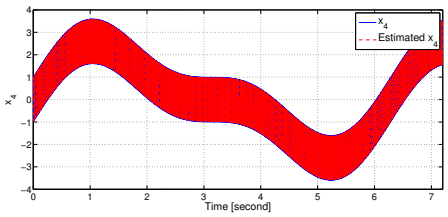

(c) Estimation performance of $d = x_4$

Fig. 8. Simulation results of case 2

[2] W. Kim and C. C. Chung, "Robust high order augmented observer based control for nonlinear systems," in *Proc. IEEE Conf. Dec. Control,* 2012, pp. 919-924.

[3] C. Kinney, R. de Callafon, E. Dunens, R. Bargerhuff, and C. Bash, "Optimal periodic disturbance reduction for active noise cancelation," *J. Sound Vib.,* vol. 305, no. 1-2, pp. 22-33, 2007.

[4] X. Chen and M. Tomizuka, "A minimum parameter adaptive approach for rejecting multiple narrow-band disturbances with application to hard disk drives," *IEEE Trans. Control Syst. Technol.,* vol. 20, no. 2, pp. 408-415, 2012.

[5] X. Chen and M. Tomizuka, "Overview and new results in disturbance observer based adaptive vibration rejection with application to advanced manufacturing," *International J. Adap. Control & Signal Processing,* to appear.

[6] B. A. Francis and W. M. Wonham, "The internal model principle of control theory," *Automatica,* vol. 12, no. 5, pp. 457-465, 1976.

[7] F. Ben-Amara, P. T. Kabamba,and a. G. Ulsoy, "Adaptive sinusoidal disturbance rejection in linear discrete-time systems part I:theory," *ASME J. Dyn. Syst. Meas. Control,* vol 121, no. pp. 648-654., 1999.

[8] W. Kim, H. Kim, C. Chung, and M. Tomizuka, "Adaptive output regulation for the rejection of a periodic disturbance with an unknown frequency," *IEEE Trans. Control Syst. Technol.,* vol. 19, no. 5, pp. 1296-1304, 2011.

[9] X. Chen and M. Tomizuka, "Selective model inversion and adaptive disturbance observer for time-varying vibration rejection on an active-suspension benchmark,"*European J. Control,* vol. 19, no. 4, pp. 300-312, 2013.

[10] Z.-P. Jiang and Y. Wang, "Input-to-state stability for discrete-time nonlinear systems," *Automatica,* vol. 37, no. 6, pp. 857-869, 2001.

[11] X. Chen and M. Tomizuka, "New repetitive control with improved steady-state performance and accelerated transient," *IEEE Trans. Control Syst. Technol.,* vol. 22, no. 2, pp. 664-675, 2014.

[12] A. Weinmann, *Uncertain Models and Robust Control,* Springer-Verlag, 1991.

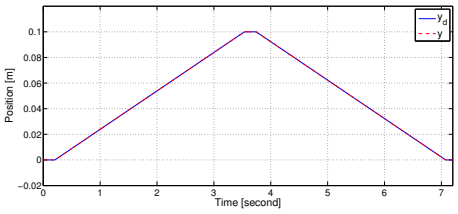

(a) Output tracking performance of y

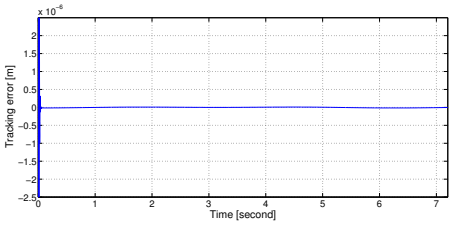

(b) Output tracking error $y_d - y$

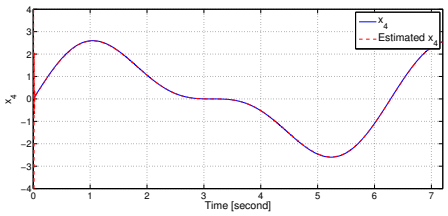

(c) Estimation performance of $d = x_4$

Fig. 9. Simulation results of case 3